Synchrony of neural Oscillators induced by random telegraphic currents

Ken Nagai and Hiroya Nakao*
Department of Physics, Kyoto University, Kyoto 606-8502, Japan

Yasuhiro Tsubo
Tamagawa University Research Institute, Tokyo 194-8610, Japan
(Received 16 November 2004; published 21 March 2005)

When a neuron receives a randomly fluctuating input current, its reliability of spike generation improves compared with the case of a constant input current [Mainen and Sejnowski, Science **268**, 1503 (1995)]. This phenomenon can be interpreted as phase synchronization between uncoupled nonlinear oscillators subject to a common external input. We analyze this phenomenon using dynamical models of neurons, assuming the input current to be a simple random telegraphic signal that jumps between two values, and the neuron to be always purely self-oscillatory. The internal state of the neuron randomly jumps between two limit cycles corresponding to the input values, which can be described by random phase maps when the switching time of the input current is sufficiently long. Using such a random map description, we discuss the synchrony of neural oscillators subject to fluctuating inputs. Especially when the phase maps are monotonic, we can generally show that the Lyapunov exponent is negative, namely, phase synchronization is stable and reproducibility of spike timing improves.

PACS number(s): 05.45.−a, 82.40.Bj, 05.40.−a

I. INTRODUCTION

It was shown by Mainen and Sejnowski in an experiment using rat neocortical slices that, when a neuron receives a randomly fluctuating input current, its reliability of spike generation improves compared with the case of a constant input current [1]. Namely, when a single neuron is driven by the same temporal sequence of a fluctuating input current, it yields very similar firing patterns at every trial, but when it is driven by a constant input current, it yields different firing patterns from trial to trial. This phenomenon has been repeatedly confirmed in many experiments, and its physiological relevance has been discussed [2,3].

From the viewpoint of nonlinear dynamics, a periodically spiking neuron driven by a constant external current is a limit-cycle oscillator [4–14]. A spike is generated when the phase of this limit cycle passes through a certain threshold value. We can interpret repeated measurements on a single neuron using the same input current as a single measurement on multiple identical neural oscillators, which are mutually independent but receive a common external input. The resulting improvement in spike timing corresponds to the phase synchronization of those uncoupled oscillators with a common external forcing. The difference in the timing of spike generation between different trials is due to the neutral stability of the limit-cycle orbit in the phase direction, in which the phase diffuses due to external disturbances. On the other hand, a neuron driven by a fluctuating input current is a random dynamical system. The improvement in spike timing implies some underlying mechanism that statistically stabilizes the limit-cycle orbit in the phase direction due to the fluctuating input. Similar situations have also been discussed

regarding synchronization of uncoupled chaotic oscillators driven by a common random forcing [15–18].

Due to the difficulty in analyzing multivariable dynamical models of neurons, most theoretical studies so far have relied upon direct numerical simulations of specific models such as the van der Pol model [8] and the FitzHugh-Nagumo model [9], or have assumed one-variable integrate-fire models or qualitative phase models of neurons [10–13]. Those studies revealed that this phenomenon can be observed commonly in a wide variety of limit-cycle oscillators that are subject to external fluctuations.

Recently, Teramae and Tanaka [14] made significant progress in understanding the universality of this phenomenon. Using the phase reduction method [4,5], they proved in general that limit-cycle oscillators always exhibit phase synchronization when they are subject to very weak Gaussian-white forcing. The standard phase reduction procedure can only be applicable when the deformation of the limit cycle is very small [4,5]. Therefore, in their analysis, fluctuation of the input was assumed to be vanishingly small, so that it did not affect the structure of the limit cycle. However, in many dynamical models of neurons, the input current is a bifurcation parameter whose variation easily leads to deformation of their limit-cycle orbits.

In this paper, we treat this problem in a different setting. In order to make a general statement about phase synchronization, we consider a simplified situation. That is, we assume the input current to be a simple random telegraphic signal that jumps between two values, and also the neuron to always be self-oscillatory. The fluctuation need not be vanishingly small. Owing to these assumptions, we can reduce the dynamics of the system to simple random maps. Though these assumptions are not physiologically realistic, they enable us to understand the phase synchronization of limit-cycle oscillators due to a common fluctuating input more generally from the viewpoint of nonlinear dynamics.

*Electronic address: nakao@ton.scphys.kyoto-u.ac.jp

II. PHASE SYNCHRONIZATION INDUCED BY FLUCTUATING CURRENTS

In this section, using the FitzHugh-Nagumo neuron model [6] as an example, we demonstrate that the reproducibility of spike timing improves even if we use a random telegraphic signal that jumps between only two values instead of taking continuous values. Let us consider the following FitzHugh-Nagumo model subject to a fluctuating input current and also to external disturbances:

$$\varepsilon \dot{u} = v + A - Bu + \xi(t),$$

$$\dot{v} = v - \frac{v^3}{3} - u + I(t) + \eta(t). \qquad (1)$$

Here, the variables u and v represent refractoriness and activation (or membrane potential) of the neuron, ε is a small dimensionless parameter that corresponds to the time constant of the refractoriness variable, and A and B are parameters. $I(t)$ represents a time-dependent input current to the neuron. $\xi(t)$ and $\eta(t)$ are Gaussian-white noises of mean 0 and variance D that are introduced to represent various external disturbances to the neuron, whose correlation functions are given by

$$\langle \xi(t)\xi(t')\rangle = D\delta(t-t'), \quad \langle \eta(t)\eta(t')\rangle = D\delta(t-t'). \quad (2)$$

We fix the parameters at $\varepsilon = 0.08$, $A = 0.7$, $B = 0.8$, and the noise strength at $D = 10^{-6}$ unless specified otherwise.

When the input current $I(t)$ takes a constant value $I(t) \equiv I_0$, this FitzHugh-Nagumo model exhibits limit-cycle oscillations for $0.33 \lesssim I_0 \lesssim 1.42$. We define the time of spike generation for this FitzHugh-Nagumo oscillator as the moment at which the variable v changes its sign from $v < 0$ to $v > 0$ on the limit cycle. We take this point as the origin, and define a phase that increases with a constant angular velocity along the limit cycle (see the next section) [4,5].

The fluctuating input current $I(t)$ is generated by a random telegraphic process, which jumps between two values I_1 and I_2 at random moments following a Poisson process [19]. If we denote by ν the probability for $I(t)$ to change its value in an infinitesimal time interval dt, the distribution $P(T)$ of the time interval T during which $I(t)$ stays at one of the two values is exponential

$$P(T) = \frac{1}{\tau}\exp\left(-\frac{T}{\tau}\right), \qquad (3)$$

where $\tau = \nu^{-1}$ represents the mean switching time of $I(t)$.

Figure 1 shows temporal evolution of an ensemble of 50 noisy FitzHugh-Nagumo oscillators described by Eq. (1) subject to a constant input current $I(t) \equiv 0.9$ [or 50 trials on a single oscillator using the same $I(t)$], where the activation variable v, the phase, the moments of spike generation, and the variance of the phase are plotted. Though all oscillators start from the same initial condition, the phases of the oscillators disperse considerably due to the external noises $\xi(t)$ and $\eta(t)$ after a long time. Correspondingly, the timing of spike generation differs considerably among the oscillators, and the variance of the phase is consistently large.
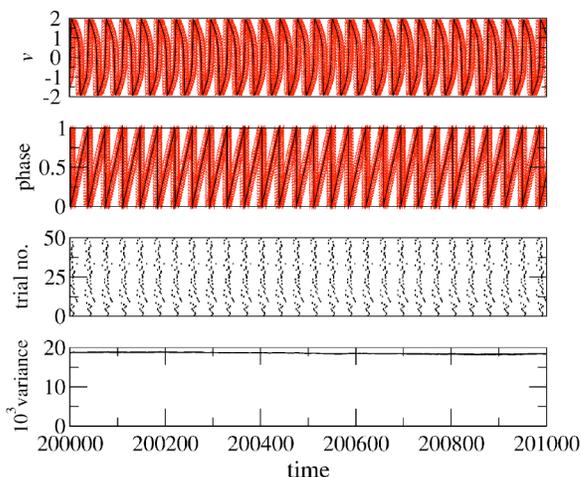
FIG. 1. Temporal evolution of activation variable v, phase, timing of spike generation, and variance of the phase for a constant input current $I(t) \equiv 0.9$. Results of 50 trials on a single FitzHugh-Nagumo oscillator (or a single trial on 50 independent oscillators) are shown in each figure, except the bottom figure.

On the other hand, Fig. 2 shows temporal evolution of the same 50 FitzHugh-Nagumo oscillators subject to a common fluctuating input current $I(t)$ that jumps between $I_1 = 0.8$ and $I_2 = 1.0$. Here, the phase defined along the limit cycle corresponding to $I(t) = I_1$ is used in drawing the figure. The switching time is set at $\tau = \nu^{-1} = 200$, which is about 5 times larger than the period of the FitzHugh-Nagumo oscillator (approximately 36.5 at $I_1 = 0.8$). In this case, dispersion of the phase is strongly suppressed. The spike timing coincides well among the oscillators, and the variance of the phase takes very small values except during several short intervals. From this figure, it is evident that the phase synchronization of the oscillators (and corresponding improvement in spike timing) occurs even if $I(t)$ takes only two values and the oscillators are always self-oscillatory.
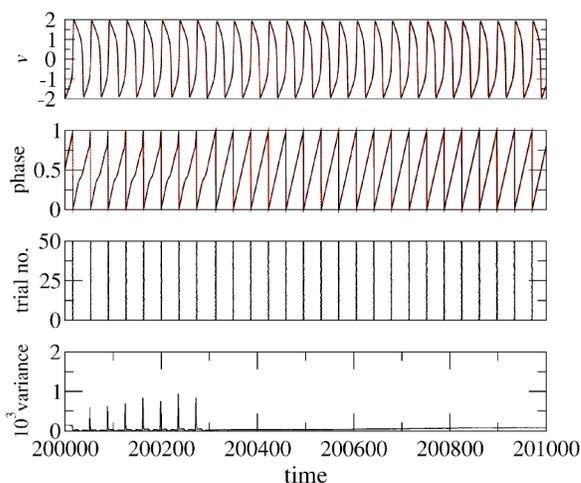
FIG. 2. Temporal evolution of activation variable v, phase, timing of spike generation, and variance of the phase for a fluctuating input current $I(t)$ that jumps between $I_1 = 0.8$ and $I_2 = 1.0$. Results of 50 trials on a single FitzHugh-Nagumo oscillator are shown in each figure, except the bottom figure.
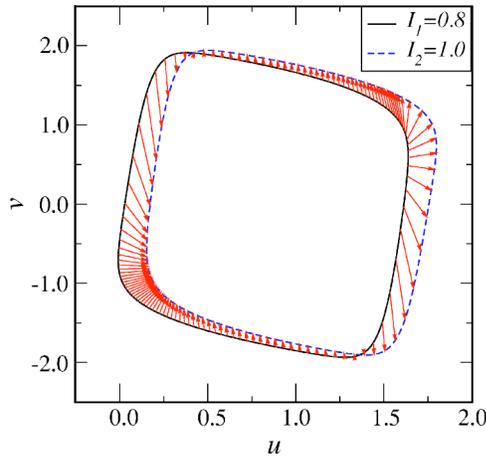
FIG. 3. Limit cycles of the FitzHugh-Nagumo model at $I(t) \equiv I_1 = 0.8$ and $I(t) \equiv I_2 = 1.0$. Points on the limit cycle 1 and their images on the limit cycle 2 are connected by arrows.

III. REDUCTION TO RANDOM PHASE MAPS

In this section, we reduce the dynamics of our limit-cycle oscillators driven by a random telegraphic current to random phase maps, and discuss its stability in the phase direction. We adopt the FitzHugh-Nagumo neuron model [Eq. (1) without the external noise terms $\xi(t)$ and $\eta(t)$] as an example, but our argument itself is generally applicable to a wide class of limit-cycle oscillators.

A. Random phase maps between limit cycles

Corresponding to two values of $I(t)$, our system jumps between two phase spaces, namely, a phase space corresponding to $I(t) = I_1$ that has a limit cycle "1" (LC1), and another phase space corresponding to $I(t) = I_2$ that has a limit cycle "2" (LC2); see Fig. 3. When the switching time τ of $I(t)$ is much larger than the relaxation time of the orbit to the limit cycle on each phase space, our system is almost always on one of the limit cycles. If a phase is defined on each limit cycle, the temporal evolution of the system can be described as an alternate phase mapping between two limit cycles.

Following standard procedure [4,5], we define two phases θ_1 and θ_2 on LC1 and LC2, respectively. Each phase increases with a constant angular velocity on its limit cycle, and is normalized by the period of the limit cycle so that its range is $[0,1]$, where 0 and 1 represent the same phase. The definition of the phase can be extended to general phase-space points that are not right on the limit cycle except phase singular points. It is achieved by identifying such a point P in the phase space with a point Q right on the limit cycle in such a way that an orbit starting from P and another starting from Q asymptotically coincide. A set of points that have equal phase is called an isochron. On the limit cycles, the phases evolve according to

$$\dot{\theta}_1 = \omega_1, \quad \dot{\theta}_2 = \omega_2, \quad (4)$$

where ω_1 and ω_2 are angular velocities of LC1 and LC2. When $I(t)$ is constant, perturbation in the phase direction is
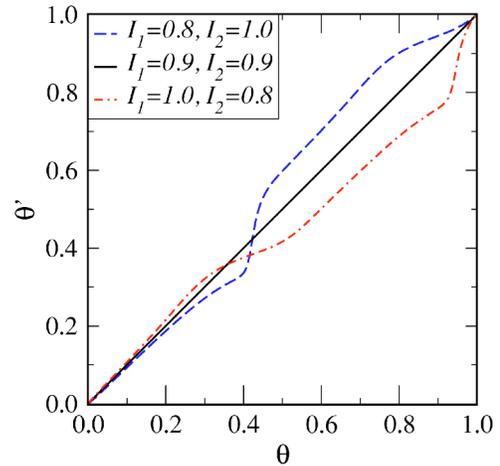
FIG. 4. Phase maps $\theta_2 = f_1(\theta_1)$ from LC1 to LC2, and $\theta_1 = f_2(\theta_2)$ from LC2 to LC1 for $I_1 = 0.8$ and $I_2 = 1.0$. Origins of the maps are shifted arbitrarily for simplicity. Trivial identity map for $I_1 = I_2 = 0.9$ is also shown.

neutrally stable. Therefore, in the presence of external disturbances, the phase perturbation gradually increases, resulting in different spike timing between trials.

Let us consider the situation in which the input current is $I(t) = I_1$ and the system has phase θ_1 on LC1. When $I(t)$ is switched to $I(t) = I_2$, the system is on a certain isochron of LC2 whose phase is θ_2, and it gradually approaches LC2. Thus, a point on LC1 at phase θ_1 is mapped to a new point on LC2 at phase θ_2. We denote this map as $\theta_2 = f_1(\theta_1)$. Similarly, we denote the map from a point on LC2 at phase θ_2 to a new point on LC1 at phase θ_1 by $\theta_1 = f_2(\theta_2)$.

Figure 3 shows LC1 and LC2 of the FitzHugh-Nagumo model at $I_1 = 0.8$ and $I_2 = 1.0$, where the mapping from LC1 to LC2 is shown by arrows. Figure 4 shows corresponding phase maps $\theta_2 = f_1(\theta_1)$ and $\theta_1 = f_2(\theta_2)$ between LC1 and LC2. For comparison, a trivial identity map for $I_1 = I_2 = 0.9$ is also shown. In drawing the maps, the origin of each limit cycle is arbitrarily shifted for simplicity so that $\theta_1 = 0$ of LC1 is mapped to $\theta_2 = 0$ of LC2 and vice versa. This does not affect the stability analysis given below.

Let us start from the moment at which $I(t)$ switches from I_1 to I_2. $I(t)$ maintains the value I_2 for a duration of T_2, then switches to I_1 and maintains this value for a duration of T_1. During this switching process, the point θ_1 on LC1 is mapped to the point $\theta_2 = f_1(\theta_1)$ on LC2 first, then it is mapped to the new point $f_1(\theta_1) + \omega_2 T_2$ on LC2 by the constant increase of the phase, Eq. (4). This point is then mapped back to the point $f_2(f_1(\theta_1) + \omega_2 T_2)$ on LC1, and finally mapped to $f_2(f_1(\theta_1) + \omega_2 T_2) + \omega_1 T_1$ by the constant increase of the phase, Eq. (4). If we denote the phase on LC1 immediately after the nth switching of $I(t)$ to I_1 as $\theta_1(n)$, and the phase on LC2 immediately after the succeeding switching of $I(t)$ to I_2 as $\theta_2(n)$, they obey

$$\theta_2(n) = f_1(\theta_1(n)) + \omega_2 T_2, \quad \theta_1(n+1) = f_2(\theta_2(n)) + \omega_1 T_1. \quad (5)$$

Since T_1 and T_2 are random numbers whose distribution $P(T)$ obeys Eq. (3), these equations describe random maps.

The time step n is roughly related to the actual time t as $n \simeq t/2\tau$, because the mean switching time is τ.

Evolution of probability density functions (PDFs) $\rho_1(\theta_1, n)$ and $\rho_2(\theta_2, n)$ of the phases θ_1 and θ_2 is given by two Frobenius-Perron equations convoluted with transition kernels that represent random shifting on LC1 and on LC2 during random durations T_1 and T_2 [20]

$$\rho_2(\theta_2, n) = \int d\theta_2' W_2(\theta_2 - \theta_2') \int d\theta_1' \delta[\theta_2' - f_1(\theta_1')] \rho_1(\theta_1', n),$$

$$\rho_1(\theta_1, n+1) = \int d\theta_1' W_1(\theta_1 - \theta_1') \int d\theta_2' \delta[\theta_1' - f_2(\theta_2')] \rho_2(\theta_2', n). \tag{6}$$

Here, W_1 and W_2 are given by

$$W_1(\theta_1) = \sum_{j=0}^{\infty} P\left(\frac{\theta_1 + j}{\omega_1}\right) \frac{1}{\omega_1}$$

$$= \frac{e^{-\theta_1/(\omega_1\tau)}}{\omega_1\tau(1 - e^{-1/(\omega_1\tau)})} \quad (0 \leq \theta_1 \leq 1),$$

$$W_2(\theta_2) = \sum_{j=0}^{\infty} P\left(\frac{\theta_2 + j}{\omega_2}\right) \frac{1}{\omega_2}$$

$$= \frac{e^{-\theta_2/(\omega_2\tau)}}{\omega_2\tau(1 - e^{-1/(\omega_2\tau)})} \quad (0 \leq \theta_2 \leq 1). \tag{7}$$

The PDFs are expected to reach stationary states $\bar{\rho}_1(\theta_1)$ and $\bar{\rho}_2(\theta_2)$ sufficiently after the initial transient stage. But, it is generally difficult to calculate these stationary PDFs analytically even if the maps f_1 and f_2 have simple functional forms. However, in the limit of large switching time τ of $I(t)$, we have $W_1(\theta_1) \to 1$ and $W_2(\theta_2) \to 1$; hence, the stationary PDFs $\bar{\rho}_1(\theta_1)$ and $\bar{\rho}_2(\theta_2)$ approach uniform distributions in the large-τ limit

$$\bar{\rho}_1(\theta_1) \to 1, \quad \bar{\rho}_2(\theta_2) \to 1. \tag{8}$$

Thus, when τ is sufficiently large, they can be approximated by uniform distributions.

B. Lyapunov exponent

Improvement in spike timing is a result of statistical stabilization of the orbit against phase perturbations. Such stability is characterized by the Lyapunov exponent of the random maps, Eq. (5). Let us consider temporal evolution of small deviations $\Delta\theta_1(n)$ and $\Delta\theta_2(n)$ from the original orbits $\theta_1(n)$ and $\theta_2(n)$. These small deviations obey the following equations in the linear regime:

$$\Delta\theta_1(n+1) = f_2'(\theta_2(n))\Delta\theta_2(n) = f_2'(\theta_2(n))f_1'(\theta_1(n))\Delta\theta_1(n),$$

$$\Delta\theta_2(n+1) = f_1'(\theta_1(n+1))\Delta\theta_1(n+1)$$

$$= f_1'(\theta_1(n+1))f_2'(\theta_2(n))\Delta\theta_2(n), \tag{9}$$

where $f_1'(\theta_1(n)) = (df_1/d\theta_1)_{\theta_1=\theta_1(n)}$ and $f_2'(\theta_2(n))$

$= (df_2/d\theta_2)_{\theta_2=\theta_2(n)}$. Thus, at large time steps n, $\Delta\theta_1(n)$ expands as

$$\left|\frac{\Delta\theta_1(n)}{\Delta\theta_1(0)}\right| = \prod_{m=0}^{n-1} |f_2'(\theta_2(m))| \cdot |f_1'(\theta_1(m))|$$

$$= \exp\left[\sum_{m=0}^{n-1} \log|f_2'(\theta_2(m))| + \sum_{m=0}^{n-1} \log|f_1'(\theta_1(m))|\right]$$

$$\simeq \exp[(\lambda_2 + \lambda_1)n], \tag{10}$$

where we introduced Lyapunov exponents of the maps f_1 and f_2

$$\lambda_1 = \langle \log|f_1'(\theta_1)|\rangle = \int_0^1 \bar{\rho}_1(\theta_1)\log|f_1'(\theta_1)|d\theta_1,$$

$$\lambda_2 = \langle \log|f_2'(\theta_2)|\rangle = \int_0^1 \bar{\rho}_2(\theta_2)\log|f_2'(\theta_2)|d\theta_2. \tag{11}$$

$\Delta\theta_2(n)$ also evolves in the same way. If the total Lyapunov exponent $\lambda = \lambda_1 + \lambda_2$ is negative, $\Delta\theta_1(n)$ and $\Delta\theta_2(n)$ shrink on average, so that the deviations from the original orbits caused by external disturbances are canceled. Thus, the value of λ gives a (local) condition for the phase synchronization between limit cycles, and improvement in spike timing.

C. Asymptotic stability in the slow switching limit

As mentioned previously, even if the functional forms of f_1 and f_2 are explicitly given, it is not easy to calculate the stationary PDFs $\bar{\rho}_1(\theta_1)$ and $\bar{\rho}_2(\theta_2)$ analytically, and the Lyapunov exponent λ which depends on them. However, when the switching time τ of $I(t)$ is sufficiently large, the stationary PDFs of the phases are nearly uniform [see Eq. (8)]. In this limit, we can obtain sufficient conditions of phase synchronization for general f_1 and f_2: *when the phase maps f_1 and f_2 are monotonic, the Lyapunov exponent λ is always nonpositive.*

For example, when they are (strictly) monotonically increasing

$$f_1'(\theta_1) > 0, \quad f_2'(\theta_2) > 0, \tag{12}$$

we can prove that λ_1 is always nonpositive as

$$\lambda_1 = \int_0^1 \log f_1'(\theta_1)d\theta_1 \leq \int_0^1 [f_1'(\theta_1) - 1]d\theta_1$$

$$= \int_0^1 f_1'(\theta_1)d\theta_1 - 1 = 0, \tag{13}$$

where we utilized the fact that $\int_0^1 f_1'(\theta_1)d\theta_1 = f_1(1) - f_1(0) = 1$ because $f_1(\theta_1)$ is a phase map. The equality holds only when $f_1(\theta_1) = \theta_1$, namely, when the phase map is a trivial identity map. The similar argument also holds for λ_2. Thus, for monotonically increasing f_1 and f_2

$$\lambda_1 \leq 0, \quad \lambda_2 \leq 0, \tag{14}$$

always holds, so that the total Lyapunov exponent $\lambda = \lambda_1 + \lambda_2$ is always nonpositive. We can also prove that λ is al-
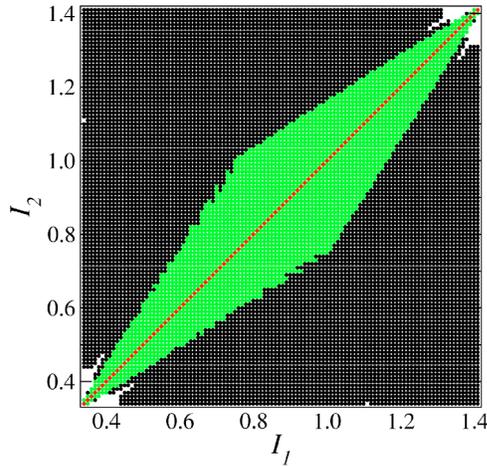
FIG. 5. Phase diagram of the FitzHugh-Nagumo model where four different domains are shown in different gray levels or colors. On the diagonal, the maps are monotonic and $\lambda \simeq 0$. In the diamond region around the diagonal, the maps are monotonic and $\lambda < 0$. In the outer regions, the maps are not monotonic but still $\lambda < 0$. In the top-right and bottom-left small regions, the maps are not monotonic and $\lambda > 0$.

ways nonpositive when the phase maps are monotonically decreasing by a similar argument. Therefore, small deviations from the original orbits always shrink by applying a slowly switching input current, when the phase maps between limit cycles are monotonic.

IV. PHASE DIAGRAMS

In this section, following our previous argument, we numerically calculate phase maps f_1 and f_2 for three different neuron models, and draw phase diagrams of phase synchronization in the I_1–I_2 plane.

A. FitzHugh-Nagumo model

First, we present results for the FitzHugh-Nagumo model. The input currents I_1 and I_2 are varied between 0.4 and 1.4. The system always exhibits limit-cycle oscillation between these values. Figure 5 displays a phase diagram of the FitzHugh-Nagumo model in the I_1–I_2 plane, where four different domains represent four combinations of (i) whether the maps f_1 and f_2 are monotonic, and (ii) the sign of the Lyapunov exponent λ calculated from f_1 and f_2 assuming uniform phase distribution. On the diagonal $I_1 = I_2$, f_1 and f_2 are trivial identity maps. In this case λ is not negative but equals zero, though f_1 and f_2 are monotonically increasing. In the diamond region around the diagonal, λ is negative from our previous discussion, because f_1 and f_2 are monotonically increasing. In the outer region, f_1 and f_2 are not monotonic but λ is still negative. In the upper-right and lower-left narrow regions, f_1 and f_2 are not monotonic, and λ is positive. Therefore, if we switch the input current in these small regions, dispersion of the phase is enhanced, and the spike timing becomes more scattered than the case of a constant input current.
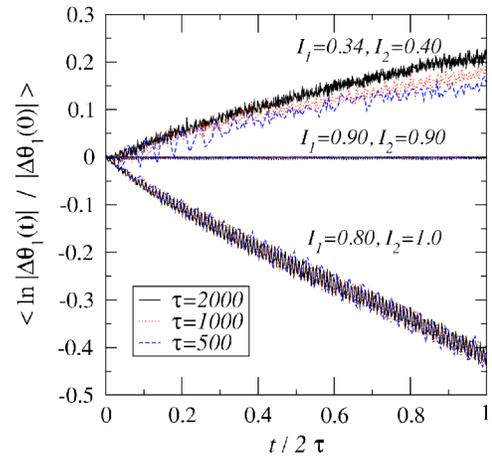
FIG. 6. Temporal evolution of small deviations in the FitzHugh-Nagumo model, where the input currents are (i) $I_1 = 0.80, I_2 = 1.0 (\lambda < 0)$; (ii) $I_1 = 0.90; I_2 = 0.90 (\lambda = 0)$; and (iii) $I_1 = 0.34, I_2 = 0.40 (\lambda > 0)$. For each pair of the input currents, three curves corresponding to $\tau = \nu^{-1} = 2000$, 1000, and 500 are plotted.

Figure 6 shows temporal evolution of small deviations $\langle \ln |\Delta\theta_1(t)/\Delta\theta_1(0)| \rangle$ that are calculated using Eq. (1) without external noises. Three pairs of input currents are chosen from three different domains in the phase diagram: (i) $I_1 = 0.80, I_2 = 1.0 (\lambda < 0)$; (ii) $I_1 = 0.90, I_2 = 0.90 (\lambda = 0)$; and (iii) $I_1 = 0.34, I_2 = 0.40 (\lambda > 0)$. The small initial deviation is set at $\Delta\theta_1(0) = 0.01\omega_1$, where the period $T_1 = \omega_1^{-1}$ of LC1 is approximately $T_1 = 36.5$ for $I_1 = 0.80$, $T_1 = 36.4$ for $I_1 = 0.90$, and $T_1 = 46.8$ for $I_1 = 0.34$. Temporal sequences of the deviation are numerically averaged over 15 000 realizations of the random telegraphic current. For each pair of the input currents, three curves corresponding to three different values of the switching time, $\tau = \nu^{-1} = 2000$, 1000, and 500, are shown. By using rescaled time $t/2\tau \simeq n$, those curves for different values of τ roughly collapse to a single curve, which indicates that our argument also holds, at least approximately, for large but finite τ. It can clearly be seen that the deviation grows, shrinks, or stays constant corresponding to the three values of the Lyapunov exponent.
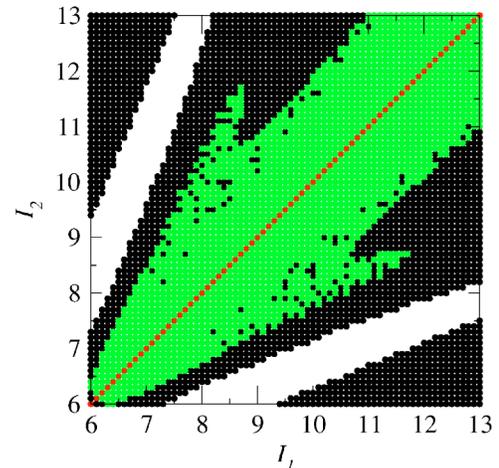
FIG. 7. Phase diagram of the Hindmarsh-Rose model. Presented in the same way as in Fig. 5.
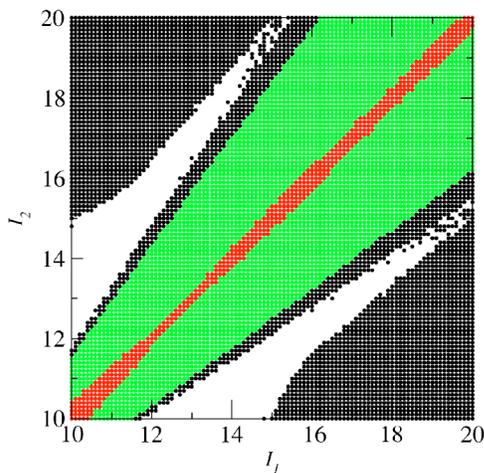
FIG. 8. Phase diagram of the Hodgkin-Huxley model. Presented in the same way as in Fig. 5.

Thus, by calculating phase maps, we can draw a phase diagram of phase synchronization. Especially in the vicinity of the diagonal where I_1 and I_2 are close, λ is always negative, and phase synchronization induced by a fluctuating input occurs. For this FitzHugh-Nagumo model, the phase synchronization also occurs in a wide parameter region, where phase maps are not monotonic. This is due to the topological constraint of this model. Since its phase space dimension is only 2, the expansion of phase difference is suppressed even if the phase maps become nonmonotonic.

B. Other neuron models

Here, we present results for the Hindmarsh-Rose model and for the Hodgkin-Huxley model of spiking neurons.

The Hindmarsh-Rose model is given by the following three-variable equations [21]:

$$\dot{x} = y - ax^3 + bx^2 + I(t) - z,$$

$$\dot{y} = c - dx^2 - y,$$

$$\dot{z} = r[s(x - x_1) - z], \tag{15}$$

where x represents membrane potential, y represents recovery variable due to fast ion channels, and the third variable z represents relaxation current due to slow ion channels that are important for burst spiking. The parameters are fixed at $a=1$, $b=3$, $c=1$, $d=5$, $r=0.006$, $s=4$, and $x_1=-1.6$. This model exhibits various self-oscillatory states for a constant input $I(t) \equiv I_0$ when $1.31 < I_0 < 25.3$.

Figure 7 displays a phase diagram of this model in the I_1-I_2 plane in the same way as Fig. 5 of the FitzHugh-Nagumo model, where I_1 and I_2 are varied between 6 and 13. As in the case of the FitzHugh-Nagumo model, the Lyapunov exponent λ is zero on the diagonal, and is negative in the vicinity of the diagonal where the phase maps are monotonically increasing. Thus, this model also possesses parameter regions where phase synchronization induced by a fluctuating input current occurs. In the outer regions the phase maps are not monotonic, and λ takes both positive and

(a)

(b)

(c)

(d)
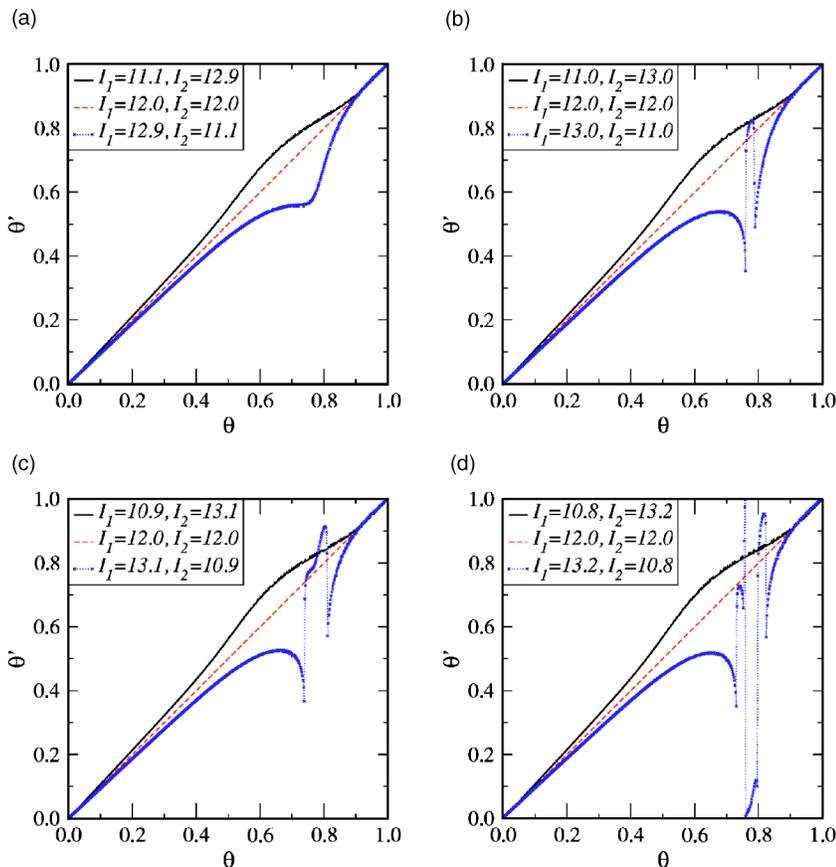
FIG. 9. Phase maps $\theta_2 = f_1(\theta_1)$ and $\theta_1 = f_2(\theta_2)$ of the Hodgkin-Huxley model for several pairs of the input currents I_1 and I_2: (a) $I_1=11.1, I_2=12.9$; (b) $I_1=11.0, I_2=13.0$; (c) $I_1=10.9, I_2=13.1$; and (d) $I_1=10.8, I_2=13.2$. Origins of the maps are arbitrarily shifted. Trivial identity map for $I_1=I_2=12$ is also shown in each figure.

(a)

(b)

(c)
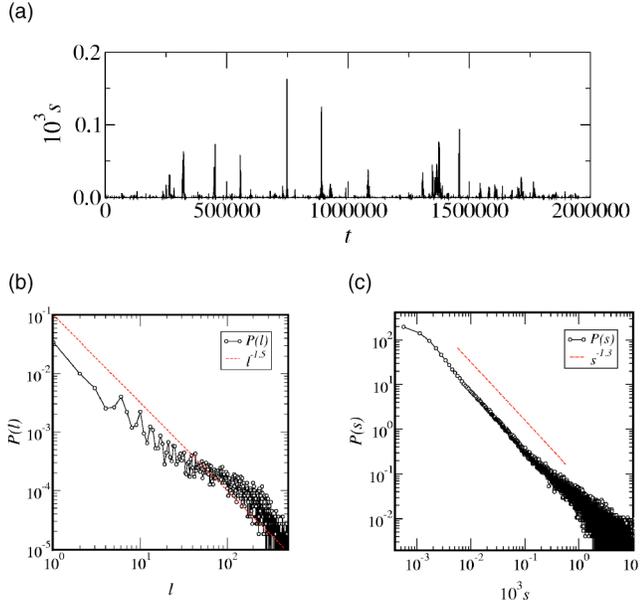
FIG. 10. Noisy on-off intermittency exhibited by an ensemble of 50 FitzHugh-Nagumo oscillators subject to a fluctuating current. Parameters are the same as that used in Fig. 2, and the noise strength is $D=10^{-7}$. (a) Temporal sequence of the phase variance $s(t)$. (b) Distribution $P(l)$ of the laminar intervals l obtained from $s(t)$. The threshold value used to separate bursts from laminar region is $s_{th}=0.5$. Theoretical power law $l^{-1.5}$ is also shown for comparison. (c) Distribution $P(s)$ of the phase variance s obtained from $s(t)$. A power-law curve $s^{-1.3}$ is also shown for comparison.

negative values. A small number of irregular points around the borders between domains are due to numerical errors. When compared with the FitzHugh-Nagumo model, there exist relatively wider regions in which the Lyapunov exponent becomes positive.

The Hodgkin-Huxley model is given by the following equations for four variables [6]:

$$C_m \dot{V} = G_{Na} m^3 h (E_{Na} - V) + G_K n^4 (E_K - V)$$
$$+ G_m (V_{rest} - V) + I(t),$$

$$\dot{m} = \alpha_m (1 - m) - \beta_m m,$$

$$\dot{h} = \alpha_h (1 - h) - \beta_h h,$$

$$\dot{n} = \alpha_n (1 - n) - \beta_n n, \qquad (16)$$

where V is the membrane potential, m and h represent activation of the sodium channel, and n represents activation of the potassium channel. Parameters G_{Na}, G_K, and G_m represent conductances of the channels, E_{Na}, and E_K represent their reversal potentials, and V_{rest} represents the rest voltage. α_x, $\beta_x(x=m,h,n)$ are rate constants that are given by the following equations:

$$\alpha_m = \frac{0.1(25-v)}{\exp\left(\dfrac{25-v}{10}\right)-1}, \quad \beta_m = 4\exp\left(-\frac{v}{18}\right),$$

$$\alpha_h = 0.07\exp\left(-\frac{v}{20}\right), \quad \beta_h = \frac{1}{\exp\left(\dfrac{30-v}{10}+1\right)},$$

$$\alpha_n = \frac{0.01(10-v)}{\exp\left(\dfrac{10-v}{10}\right)-1}, \quad \beta_n = 0.125\exp\left(-\frac{v}{80}\right). \quad (17)$$

The parameters are fixed at $G_{Na}=120$, $E_{Na}=115$, $G_K=36$, $E_K=-12$, $G_m=0.3$, $V_{rest}=10.613$, and $C_m=1.0$. Given a constant input current $I(t)\equiv I_0$, this model exhibits limit-cycle oscillation when $I_0>8.9$.

Figure 8 displays a phase diagram in the I_1–I_2 plane. I_1 and I_2 are varied between 10 and 20, where the system exhibits limit-cycle oscillation. Similarly to the two previous cases, the Lyapunov exponent λ is roughly zero on the diagonal. In the vicinity of the diagonal, the phase maps are monotonic; hence, λ is negative. In the outer region the phase maps become nonmonotonic and λ takes both positive and negative values. Due to numerical errors, borders between different domains are somewhat blurred.

Since phase-space dimensions of the Hindmarsh-Rose model and the Hodgkin-Huxley model are larger than 2, the topological constraint is less tight for these models. Thus, the maps between two limit cycles can easily be complex when they become nonmonotonic, resulting in the enhancement of phase dispersion due to fluctuating input currents. For example, Figs. 9(a)–9(d) show deformation of the phase maps of the Hodgkin-Huxley model when the input currents are varied, so that the difference between I_1 and I_2 gradually increases. At $I_1=10.8$ and $I_2=13.2$ [Fig. 9(d)], the map becomes sufficiently complex for the Lyapunov exponent λ to become positive.

V. INTERMITTENT DESYNCHRONIZATION

It can be seen from Eq. (9) that the deviations $\Delta\theta_1$ and $\Delta\theta_2$ obey random multiplicative dynamics if we take fluctuation of the multipliers into account. Thus, they are expected to exhibit characteristic behavior called on-off intermittency at long time scales [7,16,22–25]. The deviations decrease on average when $\lambda<0$. However, when small additive external noises are present in the system as in Eq. (1), they are bounded from below at the external noise level. Therefore, by random multiplication due to fluctuating currents, the phase deviations occasionally grow from this lower bound rapidly to the upper bound determined by the nonlinearity of the system, resulting in repetitive transient bursting (noisy on-off intermittency).

There have been a number of studies on this phenomenon, which have shown that the distribution $P(s)$ of the amplitude s of the deviation obeys a power law, and also that the distribution $P(l)$ of the laminar (interburst) interval l during which the fluctuation s takes values lower than a certain threshold obeys a power law of the form $l^{-1.5}$ [7,16,22–25].

Let us demonstrate this using the FitzHugh-Nagumo model, Eq. (1). If we consider an ensemble of many oscillators subject to a common external input, the phase difference

between any pair of oscillators exhibits noisy on-off intermittency. Thus, the variance of the whole ensemble of oscillators also exhibits similar temporal intermittency. Such intermittency of the distribution function is reported, e.g., by Teramae and Kuramoto [14] for globally coupled chaotic maps.

Figure 10(a) displays a temporal sequence of the phase variance $s(t)$ of 50 FitzHugh-Nagumo oscillators. The parameters are the same as those in Fig. 2, and the phase defined on LC1 is used. The variance $s(t)$ is almost always very small, indicating that the ensemble of oscillators is well synchronized in phase. However, it occasionally takes a very large value, which indicates that the ensemble exhibits burst-like desynchronization of the phases. Figures 10(b) and 10(c) display the distribution $P(l)$ of the laminar intervals and the distribution $P(s)$ of the burst amplitude s obtained from such time sequences. The characteristic power-law behavior of those distribution functions is confirmed.

VI. SUMMARY

We analyzed phase synchronization exhibited by a self-oscillatory neuron model subject to a random telegraphic input current by reducing the dynamics of the system to random maps. We proved that when the maps between limit cycles are monotonic and the mean switching time of the input current is sufficiently large, the Lyapunov exponent of the system always becomes negative, leading to phase synchronization and improvement in spike timing. This result is not restricted to a special class of neurons, but generally

holds for a wide variety of limit-cycle oscillators.

In this paper, we only treated the case in which the switching time τ is sufficiently large. We need further discussions to treat smaller τ values, for which the PDFs of the phases are generally not uniform on the limit cycles. Therefore, we need to estimate the stationary PDFs $\bar{\rho}_1(\theta_1)$ and $\bar{\rho}_2(\theta_2)$ from Eq. (6) in some way, for example, by using some kind of perturbation method. Also, we considered only a random telegraphic current in this paper, namely $I(t)$, that jumps between only two values. Generalization to the case in which $I(t)$ takes multiple or continuous values is necessary to treat experimental situations more realistically.

Phase synchronization induced by fluctuating external input seems to be a universal phenomenon that is not restricted to specific dynamical models of neurons. The paper by Teramae and Tanaka [14] generally proved this fact for a vanishingly weak external Gaussian-white forcing. In this paper, we proved this fact in a different situation, where the forcing can take only two values which are not necessarily infinitesimal. We also found that the dispersion of phases could be enhanced when the fluctuating input is not vanishingly small. A more general formulation of this problem that includes the above two situations as special cases is desirable. Studies in this direction are now in progress, and will be reported in the future.

[1] Z. F. Mainen and T. J. Sejnowski, Science **268**, 1503 (1995).

[2] R. R. de Ruyter van Stevenick, G. D. Lewen, S. P. Strong, R. Koberle, and W. Bialek, Science **275**, 1805 (1997).

[3] Y. Tsubo, T. Kaneko, and S. Shinomoto, Neural Networks **17**, 165 (2004).

[4] A. T. Winfree, *The Geometry of Biological Time* (Springer-Verlag, New York, 2001).

[5] Y. Kuramoto, *Chemical Oscillations, Waves, and Turbulence* (Springer-Verlag, Berlin, 1984).

[6] C. Koch, *Biophysics of Computation* (Oxford University Press, Oxford, 1999).

[7] A. Pikovsky, M. Rosenblum, and J. Kurths, *Synchronization* (Cambridge University Press, Cambridge, 2001).

[8] R. V. Jensen, Phys. Rev. E **58**, R6907 (1998).

[9] E. K. Kosmidis and K. Pakdaman, J. Comput. Neurosci. **14**, 5 (2003).

[10] K. Pakdaman, Neural Comput. **14**, 781 (2002).

[11] B. Gutkin, G. B. Ermentrout, and M. Rudolph, J. Comput. Neurosci. **15**, 91 (2003).

[12] J. Ritt, Phys. Rev. E **68**, 041915 (2003).

[13] J. M. Casado and J. P. Baltanás, Int. J. Bifurcation Chaos Appl. Sci. Eng. **14**, 2061 (2004).

[14] J. N. Teramae and D. Tanaka, Phys. Rev. Lett. **93**, 204103

(2004).

[15] L. M. Pecora and T. L. Carroll, Phys. Rev. A **44**, 2374 (1991).

[16] A. S. Pikovsky, Phys. Lett. A **165**, 33 (1992).

[17] P. Khoury, M. A. Lieberman, and A. J. Lichtenberg, Phys. Rev. E **54**, 3377 (1996).

[18] R. Toral, C. R. Mirasso, E. Hernández-García, and O. Piro, in *Unsolved Problems of Noise and Fluctuations*, edited by D. Abbot and L. Kiss, AIP Conf. Proc. No. 511 (AIP, New York, 2000), p. 255.

[19] C. W. Gardiner, *Handbook of Stochastic Methods* (Springer, Berlin, 1997).

[20] A. Lasota and M. C. Mackey, *Probabilistic Properties of Deterministic Systems* (Cambridge University Press, New York, 1985).

[21] J. L. Hindmarsh and R. M. Rose, Nature (London) **296**, 162 (1982); Proc. R. Soc. London, Ser. B **221**, 87 (1984).

[22] H. Fujisaka and T. Yamada, Prog. Theor. Phys. **74**, 918 (1985).

[23] A. Čenys, A. N. Anagnostopoulos, and G. L. Bleris, Phys. Lett. A **224**, 346 (1997).

[24] H. Nakao, Phys. Rev. E **58**, 1591 (1998).

[25] J. N. Teramae and Y. Kuramoto, Phys. Rev. E **63**, 036210 (2001).